

PAPER • OPEN ACCESS

Quantum dot interactions with and toxicity to *Shewanella oneidensis* MR-1

To cite this article: Anna M Wroblewska-Wolna *et al* 2020 *Nanotechnology* **31** 134005

View the [article online](#) for updates and enhancements.



IOP | ebooks™

Bringing you innovative digital publishing with leading voices to create your essential collection of books in STEM research.

Start exploring the collection - download the first chapter of every title for free.

Quantum dot interactions with and toxicity to *Shewanella oneidensis* MR-1

Anna M Wroblewska-Wolna¹, Andrew J Harvie^{2,4}, Sam F Rowe³,
Kevin Critchley², Julea N Butt³  and Lars J C Jeuken^{1,5} 

¹ School of Biomedical Sciences, University of Leeds, Leeds, United Kingdom

² School of Physics and Astronomy, University of Leeds, Leeds, United Kingdom

³ School of Chemistry and the School Biological Sciences, University of East Anglia, Norwich, United Kingdom

E-mail: L.J.C.Jeuken@leeds.ac.uk

Received 19 September 2019, revised 10 November 2019

Accepted for publication 6 December 2019

Published 14 January 2020



CrossMark

Abstract

Combining abiotic photosensitisers such as quantum dots (QDs) with non-photosynthetic bacteria presents an intriguing concept into the design of artificial photosynthetic organisms and solar-driven fuel production. *Shewanella oneidensis* MR-1 (MR-1) is a versatile bacterium concerning respiration, metabolism and biocatalysis, and is a promising organism for artificial photosynthesis as the bacterium's synthetic and catalytic ability provides a potential system for bacterial biohydrogen production. MR-1's hydrogenases are present in the periplasmic space. It follows that for photoenergised electrons to reach these enzymes, QDs will need to be able to enter the periplasm, or electrons need to enter the periplasm via the Mtr pathway that is responsible for MR-1's extracellular electron transfer ability. As a step towards this goal, various QDs were tested for their photo-reducing potential, nanotoxicology and further for their interaction with MR-1. CdTe/CdS/TGA, CdTe/CdS/Cysteamine, a commercial, negatively charged CdTe and CuInS₂/ZnS/PMAL QDs were examined. The photoreduction potential of the QDs was confirmed by measuring their ability to photoreduce methyl viologen with different sacrificial electron donors. The commercial CdTe and CuInS₂/ZnS/PMAL QDs showed no toxicity towards MR-1 as evaluated by a colony-forming units method and a fluorescence viability assay. Only the commercial negatively charged CdTe QDs showed good interaction with MR-1. With transmission electron microscopy, QDs were observed both in the cytoplasm and periplasm. These results inform on the possibilities and bottlenecks when developing bionanotechnological systems for the photosynthetic production of biohydrogen by MR-1.

Keywords: quantum dots, toxicity, bacteria, light harvesting, artificial photosynthesis

(Some figures may appear in colour only in the online journal)

1. Introduction

Inorganic–biological hybrid systems have the potential to be sustainable and versatile chemical platforms through integrating the synthetic potential of bacteria and light-harvesting abilities of semiconductor nanoparticles. Given historical fossil fuel crises, superseded now by global warming and ever-growing environmental pollution, scientists endeavour to utilise bacteria to produce value-added chemicals and biofuels for the sake of global society [1, 2]. Inorganic–biological hybrid devices attempt to mimic natural photosynthesis that

⁴ Current address: Department of Chemistry, Norwegian University of Science and Technology, Trondheim, Norway.

⁵ Author to whom any correspondence should be addressed.



Original content from this work may be used under the terms of the [Creative Commons Attribution 3.0 licence](https://creativecommons.org/licenses/by/3.0/). Any further distribution of this work must maintain attribution to the author(s) and the title of the work, journal citation and DOI.

sustains CO₂ conversion, and thus they are sometimes referred to as artificial photosynthetic systems. Alternatively, efforts have been made to produce biohydrogen, which is regarded as one of the most promising energy carriers [3, 4], because it has a high energy density and is carbon-free. Despite that, and the numerous attempts that have been undertaken to optimise biohydrogen production, there is significant room for improvement.

Investigated here, *Shewanella oneidensis* MR-1 (MR-1) is a facultative anaerobe and Gram-negative bacterium. Extensive research has been invested in the characterisation of MR-1's membrane proteins that are responsible for its extracellular electron transport (EET). One extensively characterised EET protein complex is the outer membrane protein complex, MtrCAB. During exoelectrogenic respiration, electrons from the quinone pool in the inner membrane are transferred to tetraheme cytochrome, CymA, and then further transported to either small tetraheme cytochrome (STC) and/or flavocytochrome fumarate reductase (FccA) in the periplasm before finally being transferred to MtrCAB [5]. MtrA is a decaheme cytochrome located within the outer membrane transmembrane β -barrel membrane protein, MtrB. MtrA protrudes into the periplasm where it collects electrons from STC or FccA and traffics them to the extracellular lipoprotein and decaheme MtrC [6, 7].

It has been shown that the extracellular electron transfer pathway in MR-1 can be reversed in microbial electrochemical systems when a sufficiently reducing potential is applied to the solid electrode [8, 9], and under electron acceptor limited conditions [10, 11]. Electron influx into MR-1 has been recently exploited by Tefft *et al* for the synthesis of value-added chemicals such as 2,3-butanediol from acetoin [12]. These authors engineered MR-1 by introducing proteorhodopsin and butanol dehydrogenase. Illuminated by green light-emitting diodes, proteorhodopsin acted as a photosensitiser that produced a proton-motive force, driving the reverse reaction of nicotinamide adenine dinucleotide reduction (NAD⁺ to NADH) by quinol. The lipophilic quinone is reduced by an extracellular electrode via the Mtr pathway. Finally, NADH is used by butanediol dehydrogenase to catalyse the acetoin to butanediol reaction [12]. The attained results, the production of 2,3-butanediol in modified MR-1 cells, provides a proof of concept that electrons can be introduced from the electrode to not only the periplasm, but also the cytoplasm of MR-1.

Not only MR-1 is exploited in photosynthetic-like reactions but also, for example, genetically modified *Saccharomyces cerevisiae* has been shown to harvest photoexcited electrons from semiconductor nanoparticles (NPs), indium phosphide, for energy-efficient production of a shikimic acid [13].

One of the most prominent advantages of nanoscale materials (over, for instance, macroscopic electrode materials) is their high surface to volume ratio. This feature amplifies their interface interaction with biological, chemical and physical environments [14–18]. Prominent examples of NPs include carbon nanotubes, a variety of gold nanostructures and fluorescent semiconductor NPs, known as quantum dots

(QDs) [9–11]. Multiple semiconductor QD systems have been utilised as promising photosensitisers for harvesting solar energy [19, 20]. Powered by sunlight, electrons from photosensitisers can reduce chemicals of interest in solution or even in bacterial or fungal cells [13, 21–23]. These systems can thus produce value-added substances with efficiencies that are comparable to nature. For instance, fed by cadmium ions and cysteine, *Moorella acetica* synthesised CdS QDs and deposited them on its surface. Sakimoto *et al* showed that sunlight excites electrons in these CdS QDs, which are transferred to the non-photosynthetic *Moorella* to stimulate acetic acid production [23].

In a different approach, NPs are used to enhance electrical interaction between anodes and bacteria for microbial-fuel cell applications. A three-dimensional graphene aerogel anode with inoculated MR-1 decorated with Pt NPs generated a power density of 1460 mW m⁻², which is over six times larger than a carbon cloth electrode [24].

While NPs offer many advantages as illustrated above, they are not without drawbacks. The potential for NP toxicity to the microorganism is a concern. Because worldwide production and accumulation of NPs are increasing rapidly, it is inevitable that NPs will be widely released into the environment and hence, the field of nanotoxicology has received intense interest [25, 26]. For instance, sunscreens that contain TiO₂ NPs are not toxic to humans, but they might be detrimental to other organisms such as fish and bacteria due to titanium dissolution [27–29]. Despite three decades of research into NP toxicity, their effects are still not fully understood [17, 30], and substantial research into the nanotoxicology assessment of NPs that have already been released into the environment is missing [25, 31]. Therefore, it is essential to understand and evaluate how NPs might interact with living organisms and what effects their presence may trigger.

Many NPs are composed of heavy metals, which, when released, can have toxic effects. However, even without toxic elements, NPs can display detrimental effects. For example, although iron is a cofactor of many proteins, iron oxide NPs are documented to damage *Escherichia coli* membranes and significantly increase the level of reactive oxygen species (ROS) [32]. The shape and size of NPs play an essential role in their interaction with microorganisms. Uneven, rough, irregular shapes contribute to the liberation of NP constituents [28]. The atoms on the corners or edges of NPs are more biologically and chemically reactive than atoms present in the core. Another crucial feature in nanotoxicology is the NP's surface chemistry and ζ potential, which has been shown to alter their toxicity [33]. The NP size can also contribute to toxicity. For example, small QDs emit higher energy photons, which may impose the destruction of biomolecules as well as enhance ROS generation [25, 34]. Additionally, surface functionalisation plays a role in defining NP toxicity too. An added layer of atoms at the QD surface introduces new chemical elements (e.g. sulfur, silicon, phosphorus, or zinc) as well as new physicochemical features [35]. All these additions alter the potential toxicity of QDs, and their effects need

to be understood to provide detailed insights into possible toxic effects.

The research presented here is aimed at the characterisation of the interaction between a variety of QDs and MR-1 together with the elucidation of photoreduction potential of QDs. A selection of QDs was tested for the nanotoxicological effects and interaction with MR-1. The photoreduction potential of the QDs and the suitability of various sacrificial electron donors (SED) was examined by determining the photoreduction of MV^{2+} to MV^+ . We have previously shown that photoreduced MV^+ can support light-driven H_2 evolution or the hydrogenation of C=C and C=O bonds in MR-1, where MV is able to diffuse into the periplasm of MR-1 and interact with relevant redox enzymes [21].

The nature of interactions between MR-1 and QDs was studied by fluorescence and electron microscopy. MR-1 is described to have either a negative or a positive surface charge [36–38]. Furukawa showed that MR-1 possesses a small negative surface charge due to the presence of lipopolysaccharide (LPS) in the outermost cell layer. Contrary, Korenevky and Beveridge argued that MR-1 has a small positive charge of about 7.6 mV under aerobic conditions [38]. In its natural marine environment, MR-1 interacts with minerals such as MnO_2 and Fe_2O_3 . These minerals possess negative zeta potential (around -20 and -40 mV, respectively) [39, 40]. In this study, QDs were synthesised with either a positive or negative ζ potential to study its effect on interaction with MR-1.

Our ultimate vision is that QDs and/or light-harvesting nanoparticles interact with the MtrCAB to inject ‘photoelectrons’ into MR-1 for biofuel production. We have previously shown that dye-sensitised TiO_2 NPs are able to adsorb onto and efficiently photoreduce MtrC [41, 42], while carbon QDs transiently interact with proteoliposomes containing MtrCAB, transferring electrons across the lipid membrane and photoreduce encapsulated dyes [43].

2. Materials and methods

Unless otherwise stated all materials were purchased from Sigma-Aldrich or Fisher Scientific (UK). All chemicals were used as received. Analytical grade reagents were prepared using MilliQ™ water (resistivity $18.2 M\Omega\text{ cm}$, Millipore). ‘Commercial’ CdTe QDs were purchased from PlasmaChem GmbH (Rudower Chaussee 29, D-12489 Berlin, Germany). Propidium iodide (PI) was obtained from Thermo Fisher. Malvern Zeta Sizer-Nano Series- Zen 3600 was used for the ζ potential and hydrodynamic size measurements. Electronic absorbance and photoluminescence spectra were recorded on a Perkin–Elmer Model Lambda35 and Perkin–Elmer Model LS55 spectrometer, respectively.

Values are expressed as mean \pm standard deviation (SD). Paired two-tailed Student’s t-tests and ANOVA were performed using GraphPad Prism v6 (GraphPad Software, USA). Significance was defined as $p \leq 0.05$, 0.01, 0.001 and graphically presented with one, two or three stars, respectively.

Modified M-1 media [44] was used for MR-1 and *Shewanella putrefaciens* CN-32 (CN-32) growth and contained: 28 mM NH_4Cl , 1.34 mM KCl , 4.4 mM Na_2HPO_4 , 1.5 mM Na_2SO_4 , 0.7 mM $CaCl_2$, 1 mM $MgCl_2$, 5 mM PIPES (piperazine-N, N’-bis(2-ethanesulfonic acid)), a vitamin and trace element mixture. The 100 times concentrated vitamin mixture contained, per 1 l, 0.02 mg biotin, 0.02 mg folic acid, 0.1 mg pyridoxine hydrochloride, 0.05 mg thiamine hydrochloride, 0.05 mg riboflavin, 0.05 mg nicotinic acid, 0.05 mg DL-panthothenic acid, 0.05 mg p-aminobenzoic acid, 0.05 mg lipoic acid, 2 mg choline chloride, 0.01 mg vitamin B_{12} (cobalamin). The 100 times concentrated trace elements mixture contained, per 1 L, 10 mg $FeCl_2 \cdot 4H_2O$, 5 mg $MnCl_2 \cdot 4H_2O$, 3 mg $CoCl_2 \cdot 4H_2O$, 2 mg $ZnCl_2$, 0.5 mg $Na_2MoO_4 \cdot 4H_2O$, 0.2 mg H_3BO_3 , 1 mg $NiSO_4 \cdot 6H_2O$, 0.02 mg $CuCl_2 \cdot 2H_2O$, 0.06 mg $Na_2SeO_3 \cdot 5H_2O$, 0.08 mg $Na_2WO_4 \cdot 2H_2O$.

Bacterial strains were stored at $-80^\circ C$ in 25% glycerol, 25% distilled water, 50% lysogeny broth (LB) medium. Aliquots of the frozen strains were streaked on to LB-agar plates and incubated for ~ 48 h at $30^\circ C$ for MR-1 and CN-32. Single colonies were used to inoculate 10 ml of M-1 medium, which was then shaken aerobically at 200 rpm for ~ 18 h. Subsequently, the culture was used to inoculate 2 ml of M-1 in 15 ml vials. The QDs were added when bacteria entered logarithmic growth at OD_{600nm} of 0.5. Positive controls (PC) contained $50 \mu g\ ml^{-1}$ kanamycin, and negative controls (NC) containing an equal volume of 20 mM HEPES, 0.15 M NaCl, pH 7.4 (saline). As prepared samples were incubated at $30^\circ C$ and grown for 18 h with shaking at 200 rpm. Bacteria were harvested and subjected to serial dilution and spread on LB-agar and incubated at $30^\circ C$ for about 18 h. Colonies were manually counted and finally expressed as colony-forming units per one millilitre of the examined sample (CFU/ml). Experiments were repeated at least three times.

A fluorescence bacterial viability assay was used to confirm results obtained by the CFU method. Two times concentrated stock solution of propidium iodide ($60 \mu M$, PI) was prepared and stored at $-18^\circ C$ until use. The PI stock solution was mixed with bacteria solutions in a 1:1 (vol: vol) ratio and incubated for 15 min. Afterwards, samples of bacteria were placed on poly-L-Lysine coated glass slides for 15 min at $20^\circ C$. Unbound bacteria were washed away using a 0.15 M NaCl solution. Poly-L-Lysine ($MW \leq 30\ 000\ g\ mol^{-1}$) covered glass slides were prepared by 20 min incubation with $100 \mu g\ ml^{-1}$ aqueous solution of poly-L-Lysine at room temperature and washed with 0.15 M NaCl. PI-stained MR-1 was imaged with an epi-fluorescent microscope (Nikon, TiU) using 560/40 (excitation), 595 (Dichroic mirror), 630/60 (emission) filters. Image capture was performed through NIS elements software. ImageJ software was employed for image processing. Micrographs were analysed by manually counting PI and QD stained bacteria.

CdTe/CdS/TGA and CdTe/CdS/Cysteamine QDs were synthesised as described by Gaponik *et al* [45]. Briefly, the reaction employed cadmium perchlorate that was mixed with a stabilising agent, either thioglycolic acid (TGA) or cysteamine. After CdTe core growth, thiourea was added to build the QD’s shell (CdS). Immediately after the synthesis of QDs,

electronic absorbance and photoluminescence (PL) spectra were recorded and used to determine the concentration and size of nanocrystals using the method described previously [46].

Cadmium-free QDs CuInS₂ (CIS) were synthesised as described by Booth *et al* [47]. Copper and indium ions were mixed in dodecanethiol and purged with argon for 30 min. The mixture was subsequently heated from 100 °C to 220 °C and refluxed until the solution colour became dark red. A ZnS shell was synthesised by the addition of zinc stearate dissolved in octadecene and the mixture was further purged for an additional 60 min. As-synthesised CIS/ZnS QDs were hydrophobic, and so before use in biological experiments, were encapsulated in the zwitterionic polymer PMAL (poly (maleic anhydride-alt-1-decene), obtaining hydrophilic CIS/ZnS/PMAL QDs [48].

Methyl viologen assays were performed inside an N₂-filled MBraun chamber (glovebox) at <1 ppm O₂. Buffers and QD solutions were purged with nitrogen before transferring them to the glovebox. A KL5125 Cold 150 W light source (Krüss) with a 150 W (15 V) halogen lamp (Osram) and a ultraviolet (UV) filter was used in all experiments. Non-irradiated samples were treated as specified above but were covered by a dark cloth. The volume of all samples was 1 ml. The reagents were suspended in 50 mM HEPES and 50 mM NaCl, pH 7, unless otherwise stated (e.g. when MES buffer was tested for the ability to work as SED). The working concentration of MV was 0.3 mM. Concentrations of MV⁺ were quantified through the Beer–Lambert law using an extinction coefficient [49] of 42100 M⁻¹ cm⁻¹ at 396 nm or 13700 M⁻¹ cm⁻¹ at 606 nm.

To test the interaction between MR-1 and QDs, MR-1 was grown aerobically in modified M-1 media to an optical density of ~0.4 at 600 nm after which selected QDs were added at various concentrations. Cultures with QDs of 1 ml were further grown and incubated in 15 ml tubes overnight (~18 h) at 30 °C, with shaking at 200 rpm. The following day, bacteria were harvested by centrifugation (5000×g, 10 min). The supernatants were discarded and pellets resuspended in 1 ml of 20 mM HEPES, 0.15 M NaCl, pH 7.4. Centrifugation was repeated 3 times to ensure the removal of unbound QDs. Following these steps, 5–10 μl of samples were put onto poly-L-lysine coated glass slides and covered with a coverslip as described above. The prepared slides were rested for 10 min to minimise bacteria motility after which they were examined with epifluorescent microscopy. Appropriate filters were used, as indicated in the Result section.

For transmission electron microscopy experiments, MR-1 samples, after overnight incubation with either 5 μM of commercial CdTe QDs, or an equal volume of 20 mM HEPES, 0.15 M NaCl, were centrifuged 5000×g, 10 min, and fixed by 2.5% glutaraldehyde in 0.1 M phosphate buffer for 2.5 h. Samples were washed twice for 30 min with 0.1 M phosphate buffer pH 7.2 and stained with 1% osmium tetroxide in 100 mM phosphate buffer for 1 h before dehydrated using an ascending alcohol series: 20%, 40%, 60%, 80%, 2×100% for 20 min. For samples containing QDs, staining with 1% osmium tetroxide was omitted. The embedding was

performed by the two changes into propylene oxide, 20 min each, followed by transfer to embedding moulds in fresh 100% agar for 16 h incubation with shaking at temperature 60 °C. An ultramicrotome was employed to obtain the thin sections of the samples, which were imaged on a JEOL 1400 microscope and Gatan UltraScan 1000 XP CCD camera.

3. Results and discussion

3.1. Characterisation of QDs

All QDs employed here were characterised with electronic absorbance and photoluminescence spectroscopy to determine core size and concentrations (figure 1, table 1), and with dynamic light scattering to obtain the ζ potential and hydrodynamic size (table 1). The ζ potential measurements showed that CdTe/CdS/TGA and the commercial QDs were both negatively charged (table 1). The CdTe/CdS/Cysteamine and CIS/ZnS/PMAL were found to be positively charged, although CIS/ZnS/PMAL is close to neutral at pH 7.4. The synthesised (or purchased) QDs were studied for their photoreduction potential. The reduction of methyl viologen (MV) by light-irradiated QDs was monitored using various sacrificial electron donors (SED) under anaerobic conditions, as would be required for the expression of relevant proteins and enzymes in MR-1 (e.g. MtrCAB or hydrogenase). Methyl viologen has a reduction potential of –0.45 V versus the standard hydrogen electrode [49] and thus can be reduced by the QDs (see table 1 for the reduction potentials of the electronic bands of the QDs).

The assay confirmed that all QDs tested here were photoelectrochemically active and able to photo-reduce methyl viologen (figure 2), but the most effective SED varied between QDs. For instance, for CdTe/CdS/TGA or commercial CdTe QD samples, the reduced MV concentrations with MES as SED were less than half those with TEOA. In contrast, MES showed comparable levels of MV⁺ to TEOA in samples containing CdTe/CdS/Cysteamine QDs as photosensitisers, and far higher levels for CIS/ZnS/PMAL QDs. EDTA worked well for CdTe/CdS/TGA and CIS/ZnS/PMAL QDs with MV⁺ concentration of up to 5.2 μM and 2 μM, respectively. When CdTe/CdS/Cysteamine or commercial, negatively charged CdTe QDs were mixed with EDTA and irradiated, MV⁺ concentrations were not significantly different from control samples that were held in the dark (hence EDTA data is omitted in figure 2(B)). It was also observed that longer irradiation did not bring about higher MV⁺ concentrations (e.g. figures 2(A), (B) and (D)), while the MV⁺ formed is only a fraction of the total MV concentration, suggesting an equilibrium was formed. With all QDs showing comparable photoreduction potential, their effects on MR-1 viability were studied.

3.2. QD nanotoxicology

The results show that CdTe/CdS/TGA QDs have a small, but significant, toxic effect at 0.05 and 0.5 μM

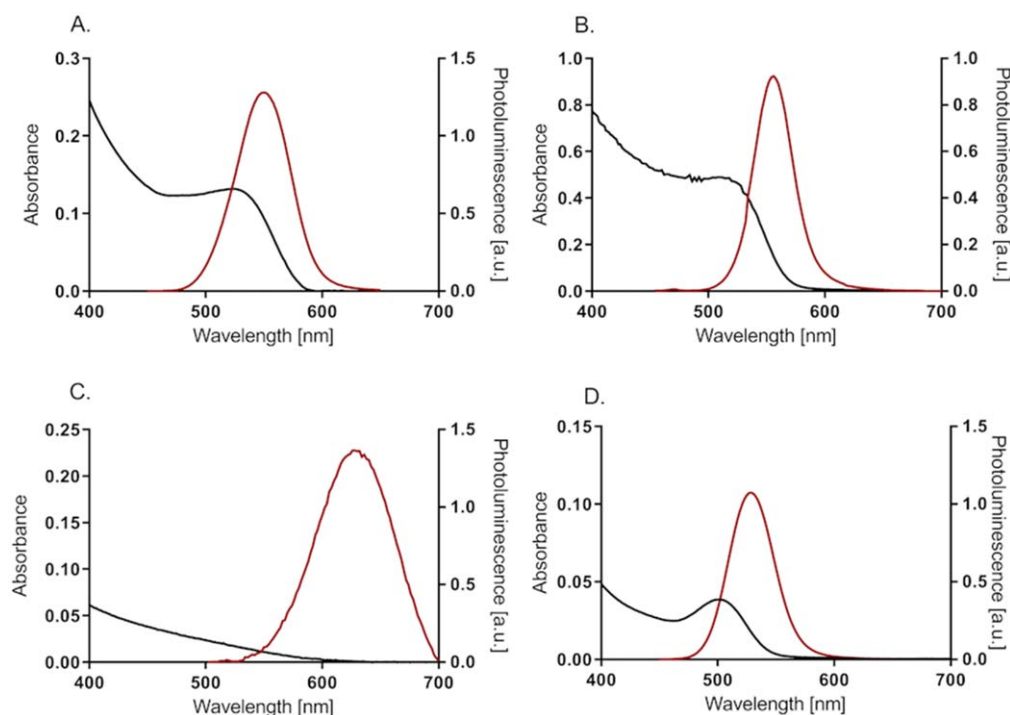
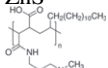
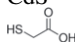
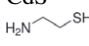


Figure 1. Absorbance (black lines, left axis) and photoluminescence (red lines, right axis) spectra of the QDs employed in this project. (A) CdTe/CdS/TGA, (B) CdTe/CdS/Cysteamine, (C) CIS/ZnS/PMAL, (D) commercial negatively charged CdTe QDs.

Table 1. Summary of key properties of QDs.

	CIS/ZnS/PMAL	CdTe/CdS/TGA	Commercial CdTe	CdTe/CdS/Cysteamine
Core, size ^a	CuInS ₂ , 2.5 nm	CdTe, 3.0 nm	CdTe, 3.0 nm	CdTe, 2.6 nm
Shell	ZnS	CdS	—	CdS
Capping ligand			Unknown	
Absorbance maximum	400 nm	525 nm	500 nm	510 nm
ϵ (M ⁻¹ cm ⁻¹) ^a	24 600	13 000	10 647	117 000
Fluorescence maximum	620 nm	550 nm	530 nm	580 nm
ζ Potential (mV)	+1.6 ± 0.3	-32.3 ± 3.7	-24.1 ± 6.0	+18.5 ± 0.2
Hydrodynamic size	12 nm (M9 media) ^b	13 nm (20 mM HEPES, pH 7.4)	15 nm (20 mM HEPES, pH 7.4)	18 nm (20 mM MES, pH 5.5)
Conduction band (V versus NHE) ^c	-0.87	-0.9	-0.9	-0.9
Valance band (V versus NHE) ^c	1.67	1.3	1.3	1.4

^a Size and extinction coefficients were calculated based on electronic and fluorescence spectra as described in [47] and [46].

^b Measured in M9 Medium, as described in [50].

^c Reduction potentials of the valance and conduction bands taken from [47, 51, 52].

(figure 3(A)). CdTe/CdS/TGA QDs were unstable and coagulated at concentrations above 5 μM in 20 mM HEPES, pH 7.4. The same concentrations (0.05–5 μM) were initially tested for CdTe/CdS/Cysteamine QDs, but even at concentrations of 0.05 μM growth was significantly inhibited and no colonies observed. To further investigate the toxicity, nanomolar concentrations of QDs were selected, e.g. 0.5, 5 and 50 nM. The CdTe/CdS/Cysteamine nanotoxicity results from $N = 3$ independent tests are presented in figure 3(B) and show that significant toxicity was observed at 50 nM NPs.

The CIS/ZnS/PMAL QDs at concentrations up to 3.4 μM do not reduce MR-1 viability (figure 3(C)). Booth *et al* previously showed that CIS/ZnS/PMAL QDs also do not decrease the viability of a human immortal keratinocyte cell line, HaCat, until concentrations went above 10 $\mu\text{g ml}^{-1}$ (equivalent to 0.34 μM) [47]. The residual toxicity of CIS/ZnS/PMAL QDs to HaCat was speculated to be mostly due to the PMAL coating [47].

Finally, the nanotoxicology studies revealed no significant toxicity for negatively charged, commercial CdTe QDs (figure 3).

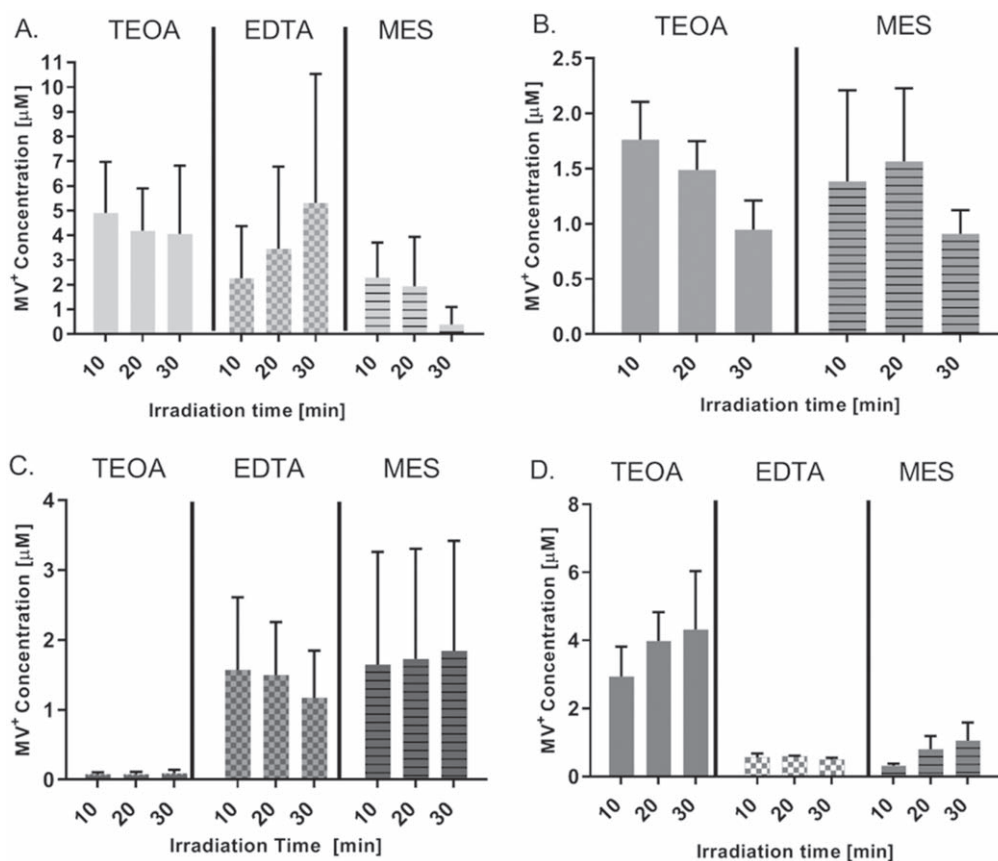


Figure 2. Photoreduction of methyl viologen (0.3 mM) using different QDs and SEDs. MV^+ concentration in μM after irradiation ($\lambda > 400$ nm, 0.7 kW m^{-2}) for times stated on the X-axes. Graph **A** depicts the results of photoreduction by 0.5 μM CdTe/CdS/TGA, **B** by 0.5 μM CdTe/CdS/Cysteamine, **C** by 2.6 μM CIS/ZnS/PMAL QDs and **D** by 1.2 μM commercial negatively charged CdTe QDs. QDs and SEDs were resuspended in 50 mM HEPES, 50 mM NaCl, pH 7, and HEPES was omitted in experiments with MES. Concentration used were 50 mM TEOA, 50 mM EDTA or MES (150 mM). MV^+ concentrations were calculated from the absorbance peak at 606 nm. Error bars represent the standard deviation for results from at least two independent experiments. Abbreviations used include TEOA—triethanolamine, EDTA—ethylenediaminetetraacetic acid, MES—2-ethanesulfonic acid.

In summary, cysteamine-coated CdTe QDs seem to have a more severe toxic effect than negatively charged particles and polymer-coatings might reduce toxicity further (we note that the supplier of the commercial QDs does not disclose the surface composition of their QDs). Next, the nature of the interaction between QDs and bacteria were visualised by fluorescence microscopy.

3.3. MR-1 interaction with the QDs

Epifluorescence microscopy revealed that CdTe/CdS/TGA QDs only interacted with a minor subpopulation of MR-1 (figure 4). Interestingly, the cells became elongated after the 18 h exposure to 0.5 μM CdTe/CdS/TGA QDs with an average length of 6.8 ± 2.9 μm ($N = 3$), about 2.5 longer than control bacteria. A similar phenomenon was also observed with 50 nM of CdTe/CdS/TGA QDs. Bacterial elongation, aka filamentation, has been documented as a reaction to environmental stress. For instance, Schneider and colleagues showed that more than 90% of MR-1 grown in LB medium supplemented with 1 μM of CdTe/TGA QDs showed an elongated cell size (at least twice longer than control) [33].

Oxidative stress experienced by bacteria is thought to inhibit cell division, increasing cell biomass [33].

As minimal interaction with MR-1 was observed, a second *Shewanella* species was tested. In comparison to other *Shewanellaceae*, CN-32 has the highest positive zeta potential [38], hence a better chance to show electrostatic binding to negatively charged CdTe/CdS/TGA QDs. The CN-32 cells were treated the same as MR-1 and visualised by epifluorescent microscopy. Like MR-1, CN-32 did not show any detectable interaction with CdTe/CdS/TGA QDs. Additionally and in contrast to MR-1, no size abnormalities were observed for CN-32 upon incubation with QDs.

As no strong interactions were observed between negatively charged CdTe/CdS/TGA QDs and MR-1, positively charged CdTe/CdS/Cysteamine QDs were tested. Very little interaction was observed at 50 nM and thus, despite its severe toxicity, MR-1 was also incubated at a higher concentration of 0.5 μM at various times. The experiment included 1, 3, and ~ 18 h incubation; however, no interaction was detected. The bacterial size increased, although to a lesser extent compared to CdTe/CdS/TGA. The bacteria became about 1.5 times longer as compared to the control bacteria that were grown without QDs.

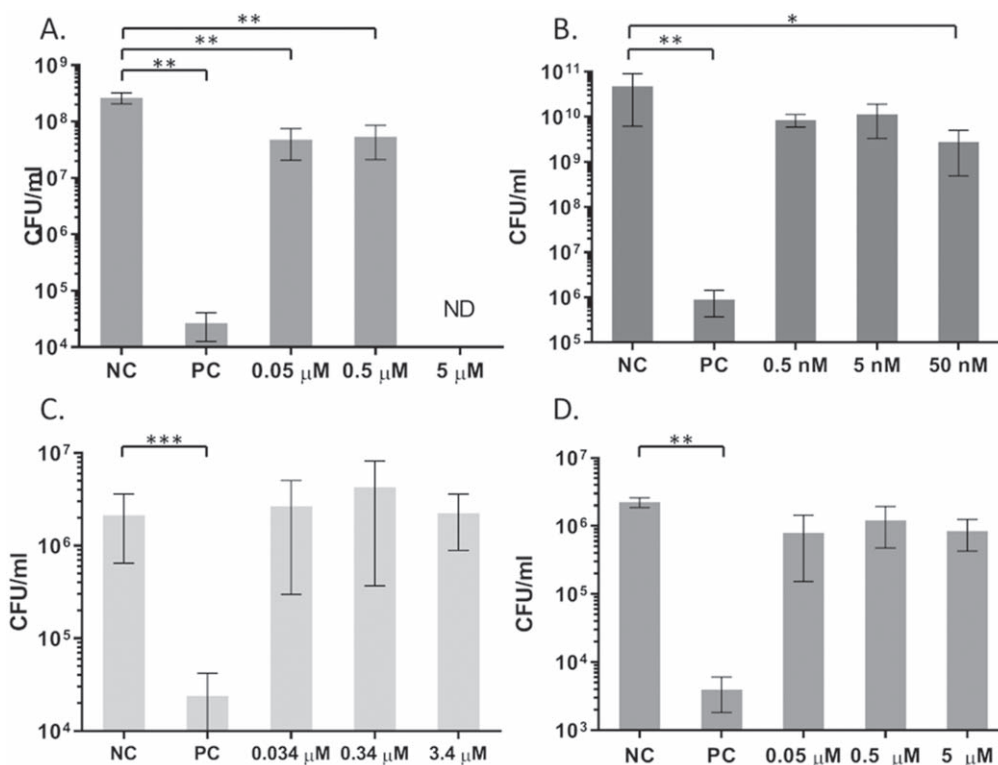


Figure 3. MR-1 viability after 18 h incubation in modified M-1 minimal media with a variety of QDs assessed by colony-forming units. Viability after incubation with (A) CdTe/CdS/TGA, $N = 4$; (B) CdTe/CdS/Cysteamine, $N = 3$; (C) CIS/ZnS/PMAL, $N = 5$ and (D) commercial negatively charged CdTe, $N = 3$. Viability is expressed in colony-forming units in 1 ml of bacteria culture (CFU ml^{-1}). NC = negative control (addition of an equal volume of 20 mM HEPES, 0.15 M NaCl, pH 7.4); PC = positive control ($50 \mu\text{g ml}^{-1}$ kanamycin).

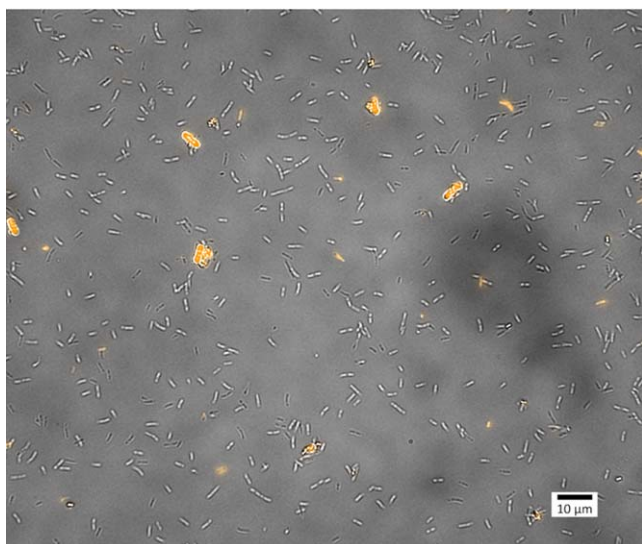


Figure 4. The representative micrograph (overlay of a bright field and a fluorescence image in orange) of MR-1 incubated for ~ 18 h with $0.5 \mu\text{M}$ of CdTe/CdS/TGA QDs. Filter sets used are excitation: 410/30, dichroic mirror 500 and emission 580/50 nm.

Since no apparent electrostatic interaction was visualised by epifluorescent microscopy, a polymer-coated QD was studied. Three concentrations of CIS/ZnS/PMAL QDs (0.034 , 0.34 , $3.4 \mu\text{M}$) were investigated, but no interaction was observed between MR-1 and the CIS/ZnS/PMAL QDs

after either 3 or ~ 18 h incubations. In contrast, epifluorescence microscopy showed clear interactions with a commercial CdTe QD, without a shell and unknown surface coating (figure 5). Live-dead fluorescence assays were performed to test whether the QDs interacted with live or dead bacteria (figure 5). Dead cells were identified by staining with propidium iodide (PI), which is a nucleic acid stain that only penetrates cells with impaired membranes (non-viable bacteria).

Three representative images of each concentration of QDs were analysed for each QD concentration after ~ 18 h incubation. 88% of a negative control (that did not contain QDs), 81%, 87% and 63% of MR-1 treated with 0.05 , 0.5 and $5 \mu\text{M}$ QDs, respectively, did not stain with propidium iodide (PI) and hence were considered viable. The low number of PI-stained bacteria confirmed our viability studies above (CFU method) and indicated that commercial CdTe QDs are not toxic to MR-1. More importantly, however, analysis of interaction and viability of MR-1 shows that a significant number of bacteria are viable (not PI stained) while interacting with commercial QDs (figure 5(B)). Importantly, the fluorescent images suggest that interaction between MR-1 and QDs is heterogeneous; only a fraction of MR-1 interacts with commercial QDs. To further localise the commercial QDs in or at the bacterial cell, transmission electron microscopy (TEM) was used.

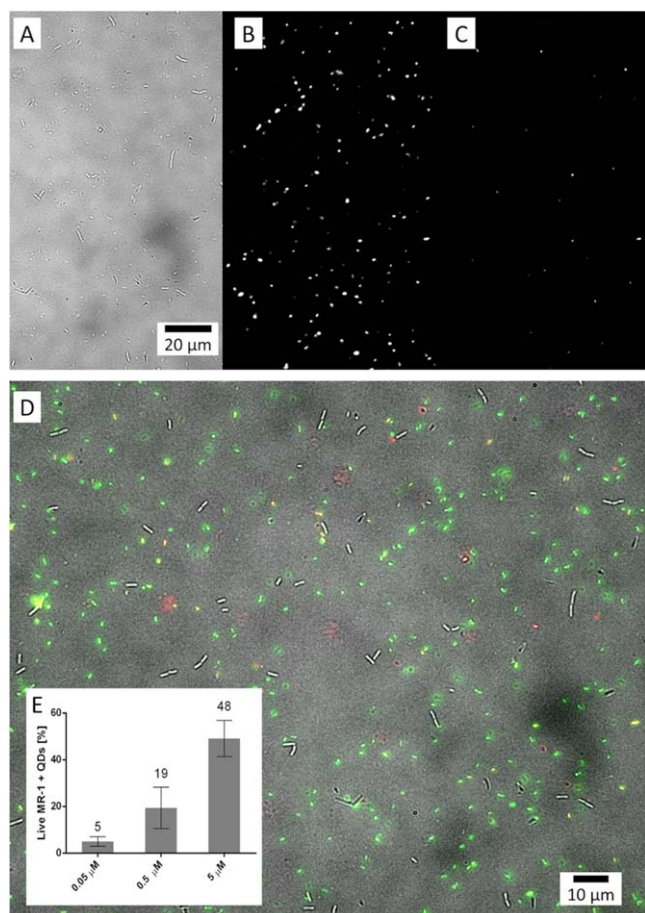


Figure 5. (A) Representative pictures MR-1 incubated for ~ 18 h with $5 \mu\text{M}$ of commercial CdTe QDs and stained with propidium iodide (PI); (A) bright field, (B) photoluminescence of commercial CdTe QD. (C) Fluorescence of propidium iodide (PI), (D) merged channels (QDs in green; PI in red; both appears as yellow). The filter settings used were (PI) excitation 560/55, dichroic mirror 595, emission 650/75 nm; (QDs) excitation 410/20, dichroic mirror 500 and emission at 535/50 nm. (E) Percentage of viable MR-1 interacting with commercial QDs ($N = 3$).

TEM images of MR-1 incubated with $5 \mu\text{M}$ commercial CdTe QDs showed electron-dense spots localised at the surface or periplasm of MR-1, as well as in the cytoplasm (figure 6(B)). Such electron-dense areas are not observed in the negative control (figure 6(A)). Furthermore, unlike the negative control, TEM of MR-1 incubated with QDs (figure 6(B)) was not stained with OsO_4 to prevent staining artefacts. Hence, we propose the electron-dense areas in figure 6(B) are due to QDs at the surface or inside MR-1. Importantly, however, the majority of bacteria displayed impaired membrane integrity as evidenced by a visual appearance of the release of cytoplasmic material (e.g. top-right figure 6(B)). Only a small number of MR-1 seemed to have intact membranes while interacting with commercial CdTe QDs. Control samples of MR-1 grown for ~ 18 h showed that 92% of bacteria had the expected, intact membrane structure, excluding the possibility that chemicals applied in the fixation procedure triggered artefacts.

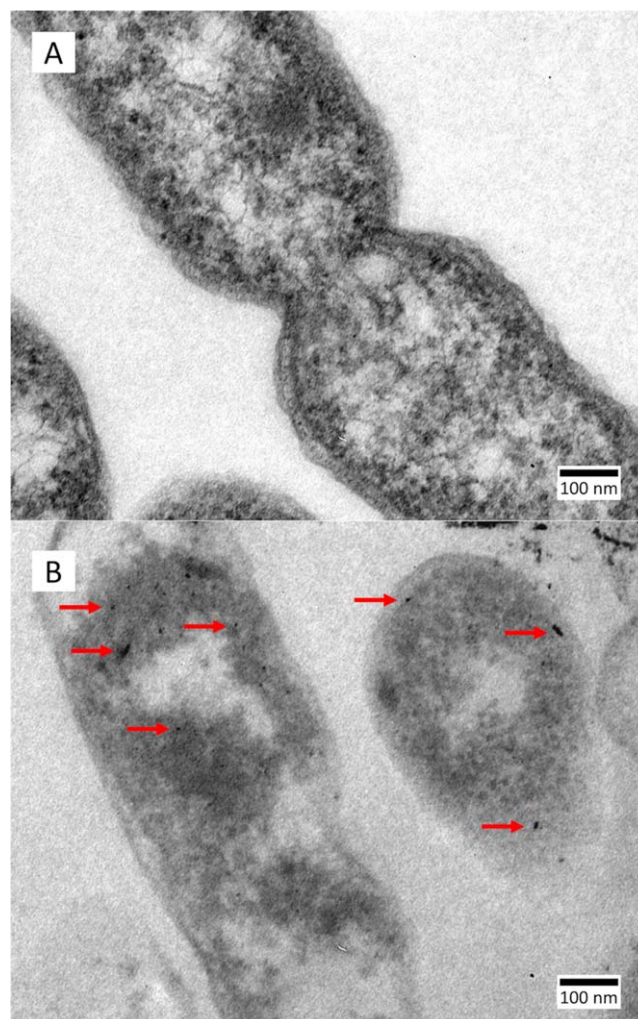


Figure 6. Representative thin-section transmission electron microscopy images of MR-1 after ~ 18 h incubation with $5 \mu\text{M}$ commercial, negatively charged CdTe QDs. (A) Negative control; (B) MR-1 incubated with QDs. Red arrows indicate the electron-dense places where it is believed cadmium-containing QDs are present.

The TEM analysis is in stark contrast to the fluorescence live-dead assay and CFU analyses, which indicated that commercial, negatively charged CdTe QD were not significantly toxic at concentrations of 0.05, 0.5 and $5 \mu\text{M}$ (see figures 3 and 5). Further studies might be able to elucidate these contradicting results (TEM versus CFU and fluorescence live-dead assay), such as the lactate dehydrogenase assay, which measures the release of the cytosolic lactate dehydrogenase enzymes. An assessment of changes in oxygen consumption by MR-1 upon commercial CdTe QDs exposure, which can be measured by respirometry, would also provide more information.

4. Conclusion

The vision of this work was to generate a background understanding to support research into the assembly of hybrid MR-1/QDs systems for biohydrogen production. The

intention was to find the least toxic nanoparticles that would interact with MR-1. For this purpose, the nanotoxicology was tested for CdTe/CdS/TGA, CdTe/CdS/Cysteamine, CIS/ZnS/PMAL and commercial, negatively charged CdTe QDs. All custom-made QDs—CdTe/CdS/TGA, CdTe/CdS/Cysteamine, and CIS/ZnS/PMAL contain an inorganic shell, which increases the longevity of the QDs in aqueous solution and moves the photoluminescence maximum towards longer wavelength. Additionally, the shell of QD prevents the liberation of toxic cadmium ions and limits ROS generation. The former was documented to be the primary way of toxicity of cadmium-containing QDs [53–55]. Low toxicity and high stability of the QDs are both critical for stimulated fuel production by MR-1. However, an inorganic shell will also create a barrier between the photooxidation sensitive core and the outside environment, reducing photo-reduction efficiency. Nonetheless, after optimisation of the SED, all QDs were able to photo-reduce MV, indicating some photo-reducing capability.

The nanotoxicology findings showed that all custom-made CdTe QDs showed moderate (e.g. CdTe/CdS/TGA) to severe (e.g. CdTe/CdS/Cysteamine) toxicity to MR-1. A significant cell elongation was observed after MR-1 was incubated with CdTe/CdS/TGA. The filamentation was also visible but to a lesser extent when bacteria were incubated with more toxic CdTe/CdS/Cysteamine QDs. Despite the clear physiological effect to MR-1, neither of the CdTe/CdS samples were observed to strongly interact with the bacteria.

Commercial negatively charged CdTe QDs, which do not contain an inorganic shell, showed no significant toxicity for MR-1 after overnight growth in modified M-1 media. The lack of toxicity was shown by the CFU method and fluorescence viability assay. In contrast to the CdTe/CdS or CIS/ZnS/PMAL QDs, the commercial QDs interacted with a subset of bacteria, the reason for which is currently unclear, although there is no preference of the QD binding either to viable or membrane-impaired bacteria. Surprisingly, TEM analysis showed that incubation with commercial QDs impaired membrane integrity, while QDs were visible inside or near the periplasm.

Acknowledgements

Funding was obtained from the UK Biotechnology and Biological Sciences Research Council (BBSRC Grants BB/K009753/1, BB/K009885/1, Doctoral Training Partnership PhD studentship to SFR), the White Rose University Consortium and the University of Leeds for funding to AMWW and AJH and AstraZeneca for a contribution to funding to AJH.

ORCID iDs

Julea N Butt  <https://orcid.org/0000-0002-9624-5226>

Lars J C Jeuken  <https://orcid.org/0000-0001-7810-3964>

References

- [1] Kornienko N, Zhang J Z, Sakimoto K K, Yang P and Reisner E 2018 *Nat. Nanotechnol.* **13** 890–9
- [2] Nocera D G 2017 *Acc. Chem. Res.* **50** 616–9
- [3] Wang H, Xu J, Sheng L, Liu X, Lu Y and Li W 2018 *Int. J. Energy Res.* **42** 3442–53
- [4] Rumpel S, Siebel J F, Farès C, Duan J, Reijerse E, Happe T, Lubitz W and Winkler M 2014 *Energy Environ. Sci.* **7** 3296–301
- [5] Mcmillan D G G, Marritt S J, Firer-sherwood M A, Shi L, Richardson D J, Evans S D, Elliott S J, Butt J N and Jeuken L J C 2013 *J. Am. Chem. Soc.* **135** 10550–6
- [6] Sturm G, Richter K, Doetsch A, Heide H, Louro R O and Gescher J 2015 *ISME J.* **9** 1802–11
- [7] Schicklberger M, Bücking C, Schuetz B, Heide H and Gescher J 2011 *Appl. Environ. Microbiol.* **77** 1520–3
- [8] Lovley D R 2012 *Annu. Rev. Microbiol.* **66** 391–409
- [9] Rowe A R, Rajeev P, Jain A, Pirbadian S, Okamoto A, Gralnick J A, El-Naggar M Y and Nealon K H 2018 *MBio* **9** e02203
- [10] Meshulam-Simon G, Behrens S, Choo A D and Spormann A M 2007 *Appl. Environ. Microbiol.* **73** 1153–65
- [11] Shi L, Belchik S M, Plymale A E, Heald S, Dohnalkova A C, Sybirna K, Bottin H, Squier T C, Zachara J M and Fredrickson J K 2011 *Appl. Environ. Microbiol.* **77** 5584–90
- [12] Tefft N M and TerAvest M A 2019 *ACS Synth. Biol.* **8** 1590–600
- [13] Guo J, Suástegui M, Sakimoto K K, Moody V M, Xiao G, Nocera D G and Joshi N S 2018 *Science* **362** 813–6
- [14] Sakimoto K K, Kornienko N, Cestellos-Blanco S, Lim J, Liu C and Yang P 2018 *J. Am. Chem. Soc.* **140** 1978–85
- [15] Saha K, Agasti S S, Kim C, Li X and Rotello V M 2012 *Chem. Rev.* **112** 2739–79
- [16] Daniel M C M and Astruc D 2004 *Chem. Rev.* **104** 293–346
- [17] Fadeel B and Garcia-Bennett A E 2010 *Adv. Drug Deliv. Rev.* **62** 362–74
- [18] Batista C A S, Larson R G and Kotov N A 2015 *Science* **350** 1242477
- [19] Kundu S, Phatthacharyya S and Patra A 2015 *Mater. Horiz.* **2** 60–7
- [20] Nabiev I, Rakovich A, Sukhanova A, Lukashev E, Zagidullin V, Pachenko V, Rakovich Y P, Donegan J F, Rubin A B and Govorov A O 2010 *Angew. Chem.—Int. Ed.* **49** 7217–21
- [21] Rowe S F et al 2017 *ACS Catal.* **7** 7558–66
- [22] Nangle S N, Sakimoto K K, Silver P A and Nocera D G 2017 *Curr. Opin. Chem. Biol.* **41** 107–13
- [23] Sakimoto K K, Wong A B and Yang P 2016 *Science* **351** 74–7
- [24] Zhao S, Li Y, Yin H, Liu Z, Luan E, Zhao F, Tang Z and Liu S 2015 *Sci. Adv.* **1** e1500372
- [25] Suresh A K, Pelletier D A and Doktycz M J 2013 *Nanoscale* **5** 463–74
- [26] Manke A, Wang L and Rojanasakul Y 2013 *Biomed. Res. Int.* **2013** 942916
- [27] Dhas S P, Shiny P J, Khan S, Mukherjee A and Chandrasekaran N 2014 *J. Basic Microbiol.* **54** 916–27
- [28] Das P, Xenopoulos A M, Williams J C, Hoque M E and Metcalfe D C 2012 *Environ. Toxicol. Chem.* **31** 122–30
- [29] Mueller N C and Nowack B 2008 *Environ. Sci. Technol.* **42** 44447–53
- [30] Wick P, Malek A, Manser P, Meili D, Maeder-Althaus X, Diener L, Diener P A, Zisch A, Krug H F and Von Mandach U 2010 *Environ. Health Perspect.* **118** 432–6
- [31] Leigh K, Bouldin J and Buchanan R 2012 *J. Toxicol.* **2012** 397657
- [32] Li Y, Yang D, Wang S, Li C, Xue B, Yang L, Shen Z, Jin M, Wang J and Qiu Z 2018 *Molecules* **23** 606

- [33] Schneider R, Wolpert C, Guilloteau H, Balan L, Lambert J and Merlin C 2009 *Nanotechnology* **20** 225101
- [34] Moos N von and Slaveykova V I 2014 *Nanotoxicology* **8** 605–30
- [35] Karakoti A S, Shukla R, Shanker R and Singh S 2015 *Adv. Colloid Interface Sci.* **215** 28–45
- [36] Furukawa Y and Dale J R 2013 *Geochem. Trans.* **14** 3
- [37] Halder S, Yadav K K, Sarkar R, Mukherjee S, Saha P, Halder S, Karmakar S and Sen T 2015 *SpringerPlus* **4** 672
- [38] Korenevsky A and Beveridge T J 2007 *Microbiology* **153** 1872–83
- [39] Carlson J J and Kawatra S K 2013 *Miner. Process. Extr. Metall. Rev.* **34** 269–303
- [40] Schütz T, Dolinská S and Mockovčiaková A 2013 *Univ. J. Geosci.* **1** 114–9
- [41] Hwang E T et al 2015 *Adv. Funct. Mater.* **25** 2308–15
- [42] Ainsworth E V et al 2016 *ChemBioChem* **17** 2324–33
- [43] Stikane A, Hwang E T, Ainsworth E V, Piper S E H, Critchley K, Butt J N, Reisner E and Jeuken L J C 2019 *Faraday Discuss.* **215** 26–38
- [44] Myers C R and Nealon K H 1988 *Science* **240** 1319–21
- [45] Gaponik N, Talapin D V, Rogach A L, Hoppe K, Shevchenko E V, Kornowski A, Eychmuller A and Weller H 2002 *J. Phys. Chem. B* **106** 7177–85
- [46] Yu W W, Qu L, Guo W and Peng X 2003 *Chem. Mater.* **15** 2854–60
- [47] Booth M, Brown A P, Evans S D and Critchley K 2012 *Chem. Mater.* **24** 2064–70
- [48] Booth M, Peel R, Partanen R, Hondow N, Vasilca V, Jeuken L J C and Critchley K 2013 *RSC Adv.* **3** 20559
- [49] Watanabe T and Honda K 1982 *J. Phys. Chem.* **86** 2617–9
- [50] Pelletier D A et al 2010 *Appl. Environ. Microbiol.* **76** 7981–9
- [51] Zhong H, Lo S S, Mirkovic T, Li Y, Ding Y, Li Y and Scholes G D 2010 *ACS Nano* **4** 5253–62
- [52] Haram S K, Kshirsagar A, Gujarathi Y D, Ingole P P, Nene O A, Markad G B and Nanavati S P 2011 *J. Phys. Chem. C* **115** 6243–9
- [53] Chen N, He Y, Su Y, Li X, Huang Q, Wang H, Zhang X, Tai R and Fan C 2012 *Biomaterials* **33** 1238–44
- [54] Rzigalinski B A and Strobl J S 2009 *Toxicol. Appl. Pharmacol.* **238** 280–8
- [55] Soenen S J, Rivera-Gil P, Montenegro J M, Parak W J, De Smedt S C and Braeckmans K 2011 *Nano Today* **6** 446–651